J Inorg Organomet Polym (2013) 23:703–711
DOI 10.1007/s10904-013-9836-7

Photoelectrochemical Sensor Based on Molecularly Imprinted Polymer-Coated TiO_2 Nanotubes for Lindane Specific Recognition and Detection

Panpan Wang · Lei Ge · Meng Li · Weiping Li · Long Li · Yanhu Wang · Jinghua Yu

Received: 24 December 2012 / Accepted: 25 January 2013 / Published online: 6 February 2013

Abstract A molecular imprinted polymer (MIP) thin film for photoelectrochemical (PEC) sensing of lindane molecules was constructed by electropolymerizing o-phenylenediamine (*o*–PD) monomer and lindane template molecule on titanium dioxide nanotubes. The resulting PEC sensors were characterized by scanning electron microscopy, ultraviolet (UV)-vis spectra and electrochemical impedance spectra. Clearly, the imprinted film showed high selectivity to lindane in our case. Under visible light irradiation, MIP film can generate the photoelectric transition from the highest occupied molecular orbital to the lowest unoccupied molecular orbital, delivering the excited electrons to the conduction band of titanium dioxide nanotubes. Simultaneously, it is believed that a positive charged hole (h^+) of MIP that took part in oxidation process was consumed to promote the amplifying photocurrent response. The MIP-based PEC sensor had an excellent specificity and could be successfully applied to the recognition and detection of lindane, indicating a promising application in handling with organochlorine pesticide.

P. Wang · L. Ge · M. Li · W. Li · L. Li · Y. Wang · J. Yu (✉)
Key Laboratory of Chemical Sensing & Analysis in Universities of Shandong, School of Chemistry and Chemical Engineering, University of Jinan, Jinan 250022, People's Republic of China
e-mail: ujn.yujh@gmail.com

Keywords Photoelectrochemical · Molecularly imprinted polymer · TiO_2 nanotubes · Lindane · Visible light

1 Introduction

The methodology of molecular imprinting, first introduced by Anderson [1], has also been well-known and widely used to produce synthetic receptors for target molecules [2, 3]. The target molecule acts as a template around which interacting and cross-linking monomers are arranged and polymerized to form a cast-like shell. After removal of the template, binding cavities that are complementary in shape, size, and position of chemical functionalities with respect to the template appear, and the resulting material can specifically recognize and bind its target.

Molecular imprinting technique for electrosynthesis of conducting polymers includes galvanostatic, potentiostatic and cyclic voltammetric methods. These provide simple and rapid techniques for controlling the thickness of the conductive polymer film, which can be easily grown and adhered to a transducer of any size and shape. Polymer thickness and deposition density, in turn, can be regulated by polymerization conditions [4]. Monomers that have been useful in the design of molecularly imprinted conducting polymers include pyrrole [5, 6], aniline, o-phenylenediamine (*o*–PD) [7, 8] and m-aminophenol [9]. In our case, *o*–PD is chosen as the functionalized monomer in the preparation of molecular imprinted polymer (MIPs). The *o*–PD monomers may be coupled in the same way as aniline during electropolymerization, producing a polymer with a polyaniline-like structure. As one of the excellent photoelectric materials, poly (o-phenylenediamine) (PoPD) has some good physical properties of higher charge carrier mobility, dissolubility, processability, and long-term

stability. Recently, electropolymerization of oPD has been reported [10]; however, to our knowledge, oPD has rarely been used in the construction of a MIPs photoelectrochemical (PEC) sensor.

PEC measurement that based on the electron transfer among analyte, semiconductor and electrode with photoirradiation is a newly developed technique for the sensing platform [11, 12]. As we known, PEC sensors exhibit some advantages of both optical methods and electrochemical sensors by coupling photoirradiation with electrochemical detection, thus in favor of promising analytical applications and provoking considerable interest [13, 14]. During the recent decades, fascinating inorganic semiconductor titanium dioxide (TiO_2) has attracted extensive attention in the photocatalytic area for decompositing organic compounds, sterilization, cancer treatment, etc. Due to its intrinsic properties involving of high photocatalytic activity, abundant resource, biological and chemical inertness, and nontoxicity [15, 16]. Although the photoelectrochemical using TiO_2 has been deeply studied for environmental protection [17–19], it is still difficult to realize the selective recognization and detection of harmful low-level pollutants in the presence of high-level less harmful pollutants. This can be ascribed to the poor selectivity of TiO_2 photocatalyst without obvious differences between these pollutants. However, MIPs can deal with this problem well.

Lindane (γ-hexachlorocyclohexane, HCH), an organochlorine pesticide, is a widely distributed contaminant [20]. Among all the HCH stereoisomers, the β–HCH [21, 22] and γ–HCH (lindane) [23] are extremely persistent and cannot be easily degraded aerobically. The persistence and organic phase solubility of HCH isomers cause significant biological accumulation and biomagnification in cells and tissues. Its well-established neurotoxicity, carcinogenicity, and consequent health risks led to a worldwide ban on use of lindane [24]. However, lindane is still found in ecological niches such as water bodies and in crops resulting in major environmental problems [25].

In this paper, utilizing molecularly imprinted PoPD film as recognition elements, a favorable selective PEC sensor was fabricated on highly ordered and vertically aligned TiO_2 NTs. It is found that the molecularly imprinted PoPD can not only work as recognition elements, but also enhance the photocurrents due to its fast electron-transfer capability and a broad and strong absorption in visible region. This strategy largely reduces the destructive effect of UV light and the photogenerated hole (h^+) of illuminated TiO_2 to template molecules. A detailed exploration for the structural, optical, and PEC properties was carried out to gain some new insights into the fundamental mechanisms. The new PoPD functionalized TiO_2 NTs (PoPD@TiO_2 NTs) has been synthesized for applying to the PEC sensing, and then a new PEC sensor has been developed for the detection of lindane by using lindane as a model.

2 Experimental Section

2.1 Apparatus and Reagents

Ti foil (0.1 mm thickness, 99.6 % purity, Goodfellow, England). Acetone, ethylene glycol and ammonium fluoride (NH_4F) were purchased from Alfa Aesar China Ltd. *o*-phenylenediamine (*o*–PD) was from Shanghai Biochemical Reagent Company (China). Lindane was obtained from Sigma-Aldrich Chemical Co. (St. Louis, MO). Ultra-pure water obtained from a Millipore water purification system (≥18.2 MΩ, Milli-Q, Millipore) was used in all assays and solutions. A 500 W Xe lamp equipped with monochromator was used as the irradiation source (CHF-XM500 W, Beijing Changtuo, China). Photocurrent was measured by the current–time curve experimental technique on a CHI 660D electrochemical workstation (Shanghai Chenhua, China) at a constant potential of 0 mV with visible light irradiation. The scanning electron microscopy (SEM) images were recorded on a QUANTA FEG 250 thermal field emission scanning electron microscopy (FEI Co., USA). UV–Visible diffuse reflectance spectra in the wavelength range from 200 to 800 nm were obtained on a UV–Visible spectrophotometer (UV-3101 spectrophotometer, SHIMADZA, Japan) equipped with an integrating sphere assembly. Fine $BaSO_4$ powders were used as a reflectance standard. All experiments were carried out at room temperature using a conventional three-electrode system with a modified TiO_2 NTs as the working electrode, a platinum wire as the auxiliary electrode, and a Ag/AgCl electrode as the reference electrode. Measurements were performed in 0.1 M phosphate buffer solution (PBS). During the PEC assay, PBS was purged with high-purity N_2 for 10 min and used as electrolyte solution. All chemicals were of analytical grade or of the highest purity available.

2.2 Fabrication of the Imprinted PoPD@TiO_2 NTs

TiO_2 NTs were prepared by anodization of titanium foils (Fig. 1b) [26]. The Ti foil was cleaned by using distilled water and acetone and dried off with N_2 gas. The bare Ti foil was anodized in an ethylene glycol solution containing NH_4F (0.38 wt%) and H_2O (1.79 wt%) and placed in a well-insulated bath for 3 h at 30 V and at 20 °C using a dc power supply (N5753A model, Agilent). The textured Ti surface was obtained by removing the first anodized TiO_2 nanotubular layer with an adhesion tape. Subsequently, the second anodization was performed for 5 min under

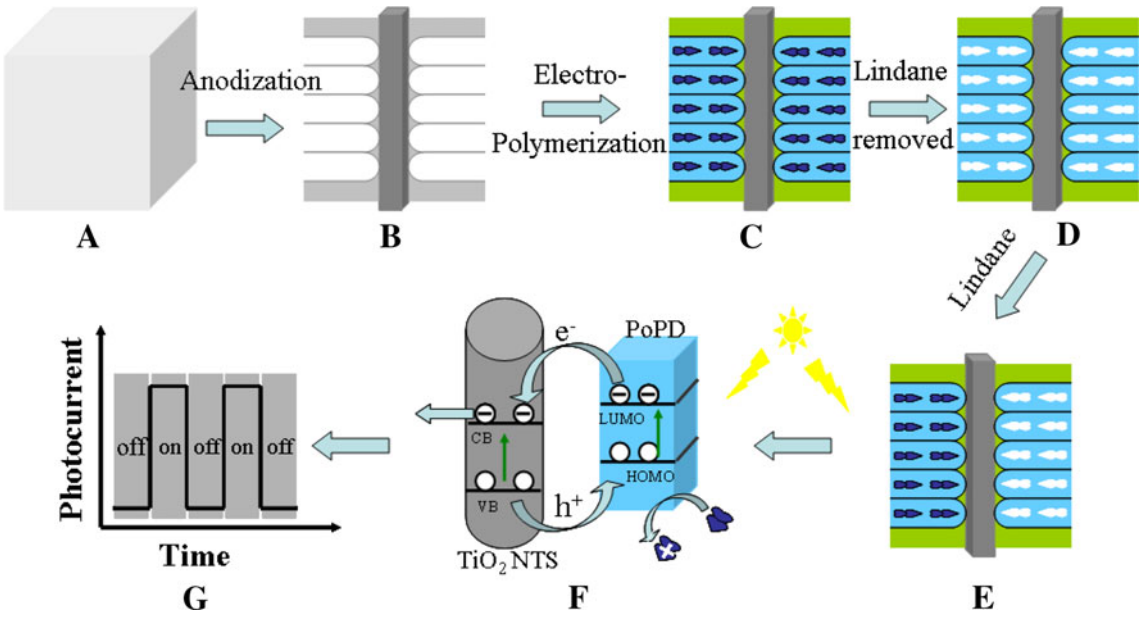

Fig. 1 Schematic illustration for fabrication (**a**, **b**, **c**, **d** and **e**) and detection mechanism (**f** and **g**) of the PEC sensor

conditions identical to those in the first anodization step. After the second anodization step, the sample was washed with distilled water and acetone and then dried off with N_2 gas. The as-formed TiO_2 NTs have an amorphous structure but the phase can be converted into anatase or rutile through annealing. Thus, thermal annealing of the anodized TiO_2 NTs was carried out 500 °C for 2 h with a heating and cooling rate of 1.7 °C/min in an ambient condition.

The film of lindane-PoPD (Fig. 1c) was prepared by electropolymerization via cyclic voltammetry scans in the range of 0–0.8 V in a HAc–NaAc (pH 5.2) buffer containing 0.05 mmol L^{-1} *o*–PD and 0.5 mmol L^{-1} template lindane at 50 mV s^{-1} for 10 cycles. In order to remove lindane, the lindane-PoPD@TiO_2 NTs were then washed five times by using Na_2CO_3 (0.1 M) solution and distilled water, respectively. Thus, the molecularly imprinted PoPD@TiO_2 NTs (Fig. 1d) were obtained and used for the following experiments. The non-imprinted PoPD@TiO_2 NTs and PoPD modified indium tin oxide coated glass electrode (POPD@ITO) were prepared as a reference in the same way without employing template molecules. Electrochemical impedance spectroscopy (EIS) was performed on an IM6x electrochemical working station (Zahner Co., Germany).

2.3 PEC and Adsorption Experiment

The PEC properties were investigated using a conventional three-electrode system in a quartz cell linked with the electrochemical workstation. The as-prepared PoPD@TiO_2 NTs were used as the working electrode. PEC experiments were performed in the quartz cell (150 mL) filled with 0.1 M pH 6.86 PBS (100 mL) at room temperature. Photocurrents were recorded in 0.1 M PBS (pH 6.86) before or after the incubation of PoPD@TiO_2 NTs in lindane solution with different concentrations for 10 min under stirring, respectively.

3 Result and Discussion

3.1 Characterization of PoPD@TiO_2 NTs

Generally, the nanotubular morphology of the substrate can provide much more multidimensional spaces for growth of conducting polymer, which is a vital factor for the development and performance of sensors. Figure 2 shows the SEM images of the prepared porous TiO_2 NTs fabricated by anodic oxidation reaction. The SEM results confirmed that the prepared TiO_2 NTs had good uniformity and high porosity on the whole (Fig. 2a). The microstructure of TiO_2 NTs gives high specific surface area and excellent space utilization, providing PoPD a wonderful substrate to grow in situ and significantly increasing the load amount of PoPD. The modification of PoPD neither completely covers the surface of TiO_2 NTs nor destroys their tubular structure, so that photocatalytic properties of TiO_2 NTs are well-retained (Fig. 2b). The elemental compositions (carbon, nitrogen, oxygen and titanium) obtained from EDS measurements are presented in Fig. 2c, which clearly indicates the presence of PoPD on the surfaces of TiO_2 NTs.

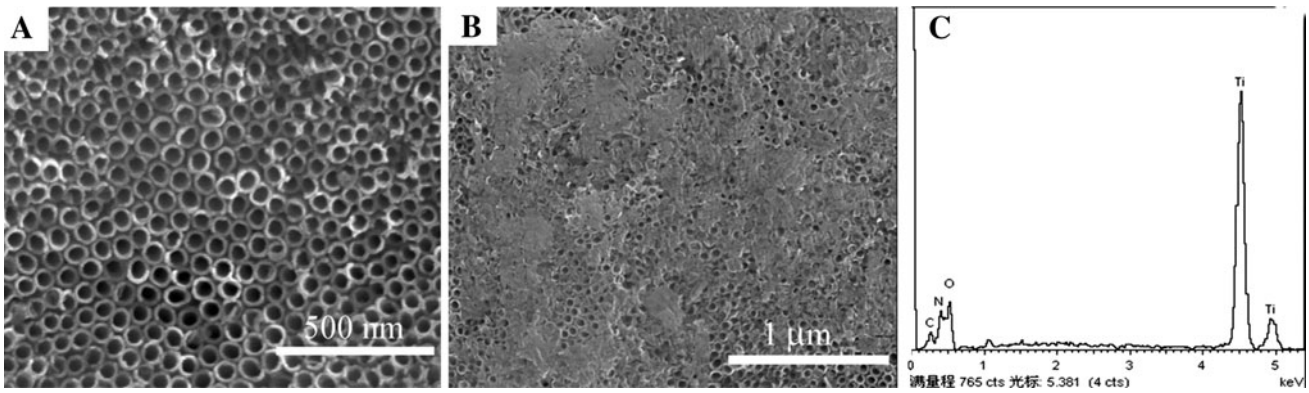

Fig. 2 SEM of TiO_2 NTs (**a**) and PoPD@TiO_2 NTs (**b**), **c** EDS spectrum of the PoPD@TiO_2 NTs electrode

The ultraviolet (UV)–Vis diffuse-reflectance spectra of the unmodified TiO_2 NTs, and PoPD@TiO_2 NTs are demonstrated in Fig. 3a, respectively. The spectra of pure TiO_2 NTs (curve a) and PoPD@TiO_2 NTs (curve c) show a very strong absorption covering the range of 300–400 nm with a peak at about 345 nm, which can be attributed to titania's strong absorption in the ultraviolet range [27, 28]. After electropolymerization of PoPD film, another two distinct adsorption peaks attributed to the adsorption peak from the PoPD itself at 295 and 475 nm (curve b) were obtained on the spectra of PoPD@TiO_2 NTs (curve c) [29]. The peak at 295 nm can be assigned to π–π* transition and that at 475 nm can be assigned to a charge-transfer exciton-like transition related to the quinoid unit which is a measure of oxidation state of the polymer. The PoPD@TiO_2 NTs showed two peaks at 280 and 460 nm. There is a 15 nm blue shift in the λ_{max} values of PoPD@TiO_2 NTs composite in comparison to the values obtained for PoPD. The blue shift was attributed to the increase in band gap due to this structural change in the polymer.

Figure 3b displays the photocurrent of TiO_2 NTs, PoPD@ITO and PoPD@TiO_2 NTs as a function of excitation wavelength at an applied potential of 0 mV in PBS (pH 6.86). It is well-known that TiO_2 is a wide band gap semiconductor material and can be excited for photocurrent generation only under UV irradiation (with wavelength below 400 nm). Bare TiO_2 NTs does not show any photocurrent above 400 nm (Fig. 3b. curve a), while PoPD@TiO_2 NTs shows photocurrent (curve c) in visible light area (400-540 nm). PoPD@ITO (curve b) shows obvious photocurrent in 400–540 nm. From the curves b and c, we can know that the biggest photocurrent were in the wavelength of 480 and 460 nm, respectively. Absorption of light by the PoPD@TiO_2 NTs induces electron transfer from the PoPD directly to the conduction band of TiO_2 and the electron was subsequently collected by the working electrode. The collected electrons are measured as photocurrent. The fast rise of the photocurrent is indicative of the efficient charge separation at the surface of the PoPD@TiO_2 NTs and good electrical communication between TiO_2 and external circuit. The changes indicated that the photocurrent in visible light area was originated from the excitation of the PoPD film. In the subsequent PEC experiments, we chose 460 nm as the excitation wavelength to investigate the maximum photocurrent only originated from PoPD@TiO_2 NTs complex.

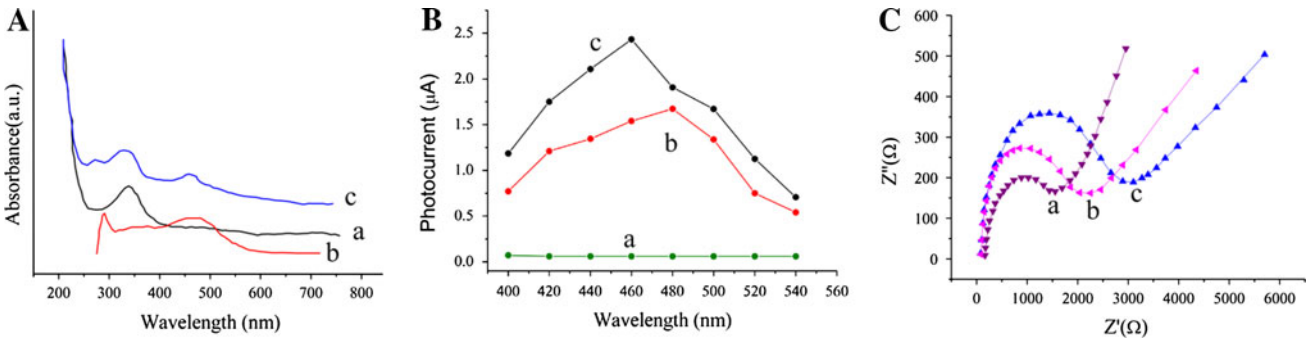

Fig. 3 (A) UV–Vis diffuse-reflection spectra of **a** TiO_2 NTs; **b** PoPD film; **c** PoPD@TiO_2 NTs. (B) Photocurrent response as a function of excitation wavelength measured in PBS (pH 6.86): **a** bare TiO_2 NTs, **b** PoPD@ITO, **c** PoPD@TiO_2 NTs. (C) AC impedance spectra of **a** TiO_2 NTs, **b** molecularly imprinted PoPD@TiO_2 NTs after and **c** before removal of lindane in 0.1 M KCl solution containing 5 mM $[Fe(CN)_6]^{3-/4-}$

Electrochemical impedance spectra (EIS) were performed to provide further evidence of interface properties and to study the electrical behaviors of the layers composing the interface. EIS were carried out in a background solution of 5 mM $[Fe(CN)_6]^{3-/4-}$ PBS. The frequency range was 100 MHz to 10 kHz. At higher frequency, the semicircle controls the interfacial electron-transfer rate of the redox-probe between the solution and the electrode, and can be used to describe the interface property of the electrode [30]. In EIS, the diameter of the semicircle at higher frequencies corresponds to the electron-transfer resistance (R_{et}); a change in the value of R_{et} is associated with the blocking behavior of the modification processes on the electrode surface, and is reflected in the EIS as a change in the diameter of the semicircle at high frequencies.

Herein, the electron-transfer of $[Fe(CN)_6]^{3-/4-}$ onto the surface of TiO_2 NTs were blocked by the formation of PoPD film on the surface of TiO_2 NTs, which resulted in an increase in R_{et}. Figure 3c shows the EIS of TiO_2 NTs at different stages of treatment. The EIS of bare TiO_2 NTs showed a relatively small R_{et} value (curve a). The R_{et} increased remarkably upon the formation of the lindane-PoPD film (curve c). This result indicates PoPD film have the larger obstruction effect, which results in reducing electron transfer rate or increasing resistance to the flow of electrons. However, after removal of lindane, the impedance (curve b) decreased accordingly. The reason may be that removal of lindane left a lot of cavities in PoPD film, and reduced the mass-transfer resistance of $[Fe(CN)_6]^{3-/4-}$ through PoPD film, and as a result accelerated the electron-transfer between the electrolyte and electrode surface. This phenomenon was consistent with literature [31].

3.2 PEC Catalysis Behavior of PoPD@TiO_2 NTs

First, photocurrent responses of molecularly imprinted PoPD@TiO_2 NTs, non-imprinted PoPD@TiO_2 NTs, and TiO_2 NTs in 0.1 M Na_2SO_4 were recorded. As illustrated in Fig. 4a, the photocurrent of the molecularly imprinted PoPD@TiO_2 NTs (curve b) and non-imprinted PoPD@TiO_2 NTs (curve c) increased evidently compared to that of TiO_2 NTs (curve a). This may result from the conjugation effect of PoPD, which can accelerate the electron-transfer and enhance the photocurrent. It was essential for improving the sensor sensibility. At the same time, the fast electron-transfer process of PoPD can effectively prevent the modified electrode from photochemical etching, and made the photoelectrochemical sensor more stable.

Secondly, photocurrent responses of the three electrodes in 0.1 M PBS (pH 6.86) without and with 1 μmol L^{-1} lindane were also studied. We could see from Fig. 4b that the photocurrent of TiO_2 NTs increased 2.1 % after addition of lindane, whereas that of non-imprinted PoPD@TiO_2 NTs and molecularly imprinted PoPD@TiO_2 NTs increased 5.7 and 14.9 %, respectively. We speculated that recognition sites on the surface of molecularly imprinted PoPD@TiO_2 NTs could specifically rebind and accumulate lindane on the electrode surface (Fig. 1e), where on the other electrodes surface lindane was nonspecifically absorbed [32, 33]. As a result, more lindane was photocatalytically oxidized on the molecularly imprinted PoPD@TiO_2 NTs, and led to a larger enhanced photocurrent. It embodied the excellent selectivity of the molecularly imprinted PoPD based photoelectrochemical sensor. It also suggested the rebinding and accumulation steps could greatly improve the sensibility of the sensor.

3.3 Optimization of Detection Conditions

After template molecules were removed from the PoPD film, the PoPD@TiO_2 NTs electrode was incubated in a stirring 2.5 μmol L^{-1} lindane for different incubation times, the photocurrent was respectively recorded in the N_2-saturated PBS (pH 6.86). The relationship between the photocurrent and the incubation time was studied in the range of 4–16 min (Fig. 4c). It can be found that the photocurrent increased rapidly in the first 10 min incubation with the increase of the incubation time. The enhancement of the photocurrent indicates that the amount of absorbed lindane in the recognition sites of PoPD film increased with the increase of the incubation time. Virtually, the photocurrent almost remained constant when the incubation time was above 10 min, implying that the adsorption equilibrium was reached on this experimental condition. Thus, the optimum incubation time should be 10 min for the determination of lindane.

The applied potential is an important parameter for producing the photocurrent. Upon PoPD@TiO_2 NTs were incubated in 1 μmol L^{-1} lindane solution for 10 min, the photocurrent sharply improved as the applied potential increasing from 0 to 0.4 V (Fig. 4d). The photocurrent at 0 mV was 40 % of that at 0.4 V, showing acceptable sensitivity for the PEC detection of lindane. To exclude the interference of other reductive species coexisting in the samples, 0 V was chosen for the PEC sensor of lindane.

3.4 PEC Detection of Lindane

Lindane detection was performed using the PoPD@TiO_2 NTs PEC sensor. Photocurrents of PoPD@TiO_2 NTs in 0.1 M PBS (pH 6.86) were recorded and demonstrated after incubating for 10 min in different concentrations of lindane (Fig. 5a and b). Under the optimum conditions, the photocurrent intensity increased linearly with the concentration of lindane over the range 0.1–10 μmol L^{-1}. The linear regression equation was calculated as

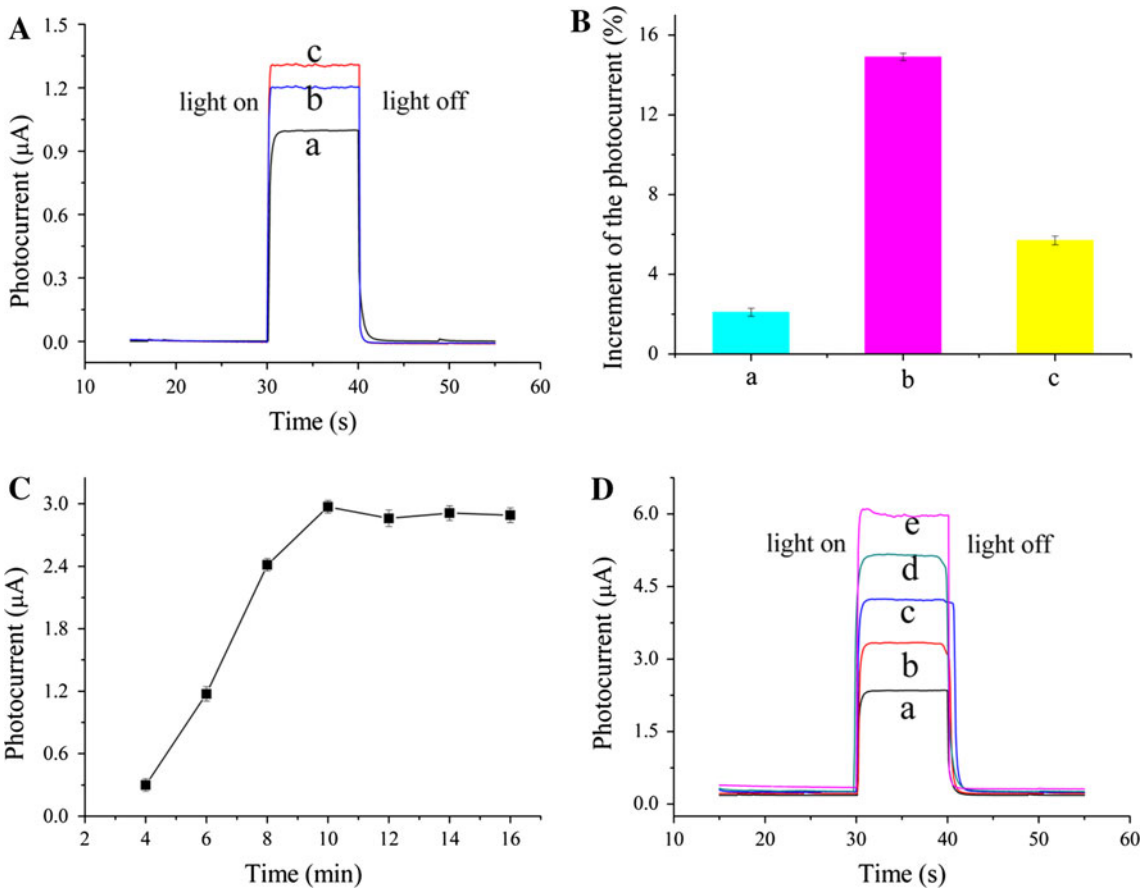

Fig. 4 (A) Photocurrent responses of **a** TiO_2 NTs, **b** the molecularly imprinted PoPD@TiO_2 NTs, and **c** non-imprinted PoPD@TiO_2 NTs measured in 0.1 M Na_2SO_4. (B) Photocurrent enhancement of **a** TiO_2 NTs, **b** molecularly imprinted PoPD@TiO_2 NTs, **c** non-imprinted PoPD@TiO_2 NTs in 0.1 M PBS (pH 6.86) after addition of 1 μmol L^{-1} lindane. (C) Effects of incubation time on photocurrent after PoPD@TiO_2 NTs incubated in 2.5 μmol L^{-1} lindane solution, where $n = 11$ for each point. (D) Effects of applied potential of 0, 0.1, 0.2, 0.3 and 0.4 V (from a to e) on the photocurrent in 0.1 M pH 6.86 PBS response of the PoPD@TiO_2 NTs after incubation in 1 μmol L^{-1} lindane for 10 min

I (μA) = 0.629 + 1.758C (μmol L^{-1}, $r = 0.998$) with a detection limit (LOD) of 0.03 μmol L^{-1} at a signal-to-noise ratio of 3σ (where σ is the standard deviation of the blank solution, each point was repeated eleven times ($n = 11$)). Table 1 shows the linear range and detection limit of pesticide with previous reports [34–36]. Compared with all the method in spite of the different analytes, this method still exhibited apparent superiority due to the new molecular imprinted-PEC detecting system. The analytical reliability and application potential of this PEC sensor was evaluated by assaying five standard lindane solution samples. The results gave the relative standard deviation (RSD) less than 5.0 %, and the recoveries are between 95.5 and 104.8 %, indicated an acceptable veracity of this method. Moreover, the response could reach the steady signal within only 10 s. Thus, the detection time of lindane was really short. Obviously, the proposed MIPs technique-based PoPD@TiO_2 NTs PEC sensor shows promise for application in the monitoring of lindane with low detection limit and short detection time.

The relative energy level of PoPD and TiO_2 NTs is shown in Fig. 1f. On the basis of PEC results, the photoelectronchemical mechanism for lindane oxidation under excitation light at 460 nm can be inferred as follows: PoPD first absorbs visible light to induce and transport electron from HOMO to LUMO, thus yielding e–h pairs. The CB of TiO_2 and PoPD match well in energy level, which can cause a synergic effect. Photogenerated electrons coming from the PoPD film were captured and injected into the CB of TiO_2 easily. The capture of the electrons in the TiO_2 separate the e–h pairs in the PoPD, hence improving the photocurrent generation efficiency. Simultaneously, h^+ in PoPD was consumed by participating in oxidation of imprinted lindane. The different transfer paths of electrons and h^+ lead to a high photoelectric conversion efficiency. From the Fig. 1f, it can be ensured that lindane was applied

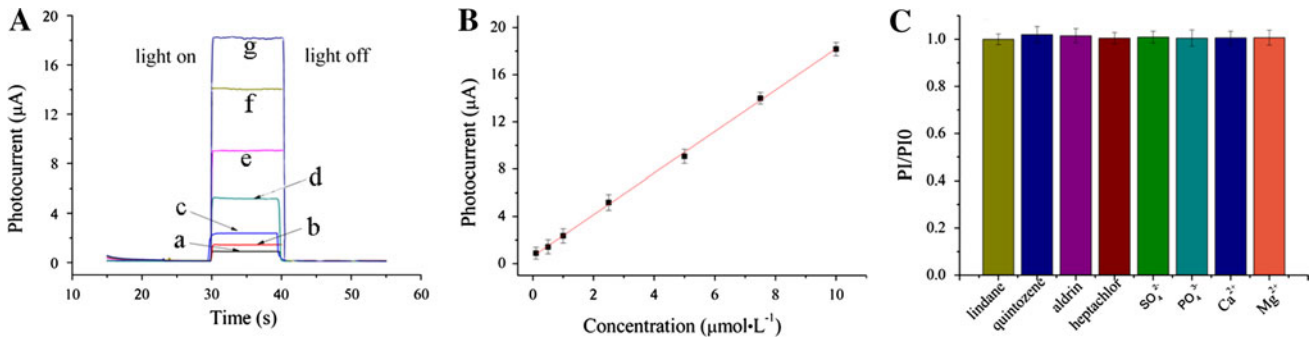

Fig. 5 (**a**) photocurrent responses at molecularly imprinted PoPD@-TiO_2 NTs electrode in 0.1 M PBS (pH 6.86) after incubation in 0.1, 0.5, 1, 2.5, 5, 7.5 and 10 μmol L^{-1} lindane (from a to g). (**b**) Linear calibration curve (eleven measurements for each point). All photocurrents were recorded in 0.1 M PBS (pH 6.86) after the electrodes were incubated in lindane solution for 10 min. (**c**) Photocurrent ration of the molecularly imprinted PoPD@TiO_2 NTs in 0.1 M PBS (pH 6.86) after incubated in 1 μmol·L^{-1} lindane in the absence (PI0) and presence (PI) of quintozene (S1), aldrin (S2), heptachlof (S3), SO_4^{2-} (S4), PO_4^{3-} (S5), Ca^{2+} (S6) and Mg^{2+} (S7) respectively

Table 1 Comparing of the proposed PEC assay protocol with other assays for determination of pesticide

Analyte	Measurement protocol	Limit of detection, linear range	Ref
Chlorpyrifos	ELISA	0.4–302, 0.07 ng L^{-1}	32
2.4-D	Molecular imprinted-electrochemical assay	1–10, 0.83 μmol L^{-1}	33
Dimethoate	Electrochemical assay	1.0–50, 0.5 ng mL^{-1}	34
Lindane	Molecular imprinted-PEC	0.1–10, 0.03 μmol L^{-1}	This work

as electron donor. An efficient electron donor can capture the h^+ in PoPD and suppress the e–h recombination, therefore generating high and stable photocurrent.

3.5 Repeatability, Stability, Selectivity and Application in Real Samples

The repeatability of the PEC sensor was evaluated by the photocurrent in 0.1 M PBS (pH 6.86) after incubation in 0.5 μmol L^{-1} lindane solution. Five sensors were prepared under the same conditions. A standard deviation (STD) of 3.11 was obtained, indicating a good sensor-to-sensor reproducibility. Moreover, the reproducibility of the sensor was examined using the 0.5 μmol L^{-1} lindane for five successive runs. The STD can be reach to 1.95.

The long-term stability of the sensor is also an important factor for practical applications. The sensor was chosen to store dry in a refrigerator (4 °C) to measure the stability. The results show that the photocurrent of the sensor after incubating in 0.5 μmol L^{-1} lindane one month later decreased by only 4.21 % compared with the initial photocurrent. Moreover, the sensor can be regenerated for the subsequent lindane detection after incubating the used PoPD@TiO_2 NTs in a lindane solution. In the current experiment, the developed sensor can be repeated approximately 50 times.

Based on the above results, the selectivity of the PEC sensor towards lindane was further investigated by employing other pesticides, oxygen-containing inorganic ions, and metal ions as interfering substances. The selectivity was evaluated by calculating the photocurrent ratio (PI/PI0), where PI and PI0 were photocurrent which were recorded in 0.1 M PBS (pH = 6.86) after the incubation of PoPD@TiO_2 NTs in lindane solution in the presence (PI) and absence (PI0) of interferences. Results (Fig. 5c) showed that 20-fold quintozene, aldrin and heptachlor hardly caused significant change of the photocurrent of lindane, where the photocurrent increased only 2.4, 2.3 and 1.7 %, respectively. 100-fold oxygen-containing inorganic ions (SO_4^{2-}, PO_4^{3-}) and 50-fold metal ions (Ca^{2+}, Mg^{2+}) had tiny influence on the determination of lindane, where the photocurrent increased only 1.1, 1.6, 0.9, 1.2 %, respectively. This phenomenon can be attributed to the application of molecular imprinting technique. It can be explained as that recognition sites formed in PoPD film could distinguish lindane from other species through molecular size and functionalized group distribution, and rebind lindane selectively by hydrogen bonds interaction. Then lindane was specifically accumulated on the surface of the PEC sensor, whereas other coexistent molecules and ions not complementary to the recognition sites and remained in the bulk solution. After washing with distilled water, lindane stays on the PoPD@TiO_2 NTs, but the interferences were removed for the nonspecific adsorption. This kind of selectivity was even more specific than that of the enzyme inhibition bioelectrochemical sensor [37]. The photocurrent variation due to the interfering substances

Table 2 Measurement results of lindane in real samples

Analyte	GC–MS* ($\mu mol\ L^{-1}$)	MIP–PEC* ($\mu mol\ L^{-1}$)	Added ($\mu mol\ L^{-1}$)	Found* ($\mu mol\ L^{-1}$)	Recovery (%)
Lindane	0.153	0.151	0.1	0.254	103
	0.155	0.153	0.3	0.448	98.3
	0.159	0.162	0.5	0.652	99.6

* Average of eleven measurements

was less than 5 % of that without interferences, indicating the selectivity of the molecularly imprinted PoPD@TiO_2 NTs PEC sensor was acceptable.

The photoelectrochemical sensor was utilized to detect lindane in spiked samples containing different pesticides or prepared with pure drinking water and river water. As shown in Table 2, the results obtained by the above method also accorded very well with those by gas chromatography-mass spectrometry (GC–MS). Recovery experiments were carried out by the proposed method. The recoveries of added lindane can be quantitative and *t*-tests showed there was no significant difference between recovery efficiency and 100 % at a confidence level of 95 %. It can be concluded that the proposed method can offer accurate results and analytical performance as good as the GC–MS. The standard deviation was all within 5 % compared to the calculated results. It indicated that the established molecularly imprinted PoPD@TiO_2 NTs PEC sensor may be used to detect real samples without pretreatment with good sensitivity and selectivity.

4 Conclusion

In this paper, the application of molecular imprinting in a thin film of an electropolymerization matrix was investigated. By incorporation of MIP, PEC sensors have shown great promise for detection of trace target molecules. The fast photoelectronic communication among lindane, PoPD, TiO_2 NTs led to a novel method for the PEC detection of lindane with good analytical performance by using lindane as a model, such as zero potential, rapid response, low detection limit, and good reproducibility and repeatability. The zero potential detection produced excellent specificity for excluding the interference of other reductive species in real samples. The molecularly imprinted PoPD@TiO_2 NTs electrode exhibits many advantages referring to the effective electronic transducer, fast response, and easy fabrication for PEC determination of lindane. In addition, this strategy largely reduces the destructive effect of UV light and the photoholes generated by illuminated TiO_2 to template molecules. Under the optimized condition, the proposed method was applied to the detection of lindane in real samples. The results were agreed with that obtained by GC–MS, indicating acceptable accuracy of the PEC sensor. The proposed molecular imprinting PEC sensor showed promising application in the monitoring of organochlorine pesticide that could donate electrons to h^+ of PoPD. Therefore, these molecular imprinting PoPD@TiO_2 NTs open a new avenue for the construction of PEC sensors.

Acknowledgments This work was financially supported by National Natural Science Foundation of People's Republic of China (No. 21277058, 21207048); Natural Science Foundation of Shandong Province, China (ZR2012BZ002); Technology Development Plan of Shandong Province, China (2011GGB01153, 2011GGX1039).

References

1. H.S. Anderson, I.A. Nicholls, Anal. Chem. **23**, 1 (2001)
2. K. Haupt, K. Mosbach, Chem. Rev. **100**, 2495 (2000)
3. J. Matsui, M. Higashi, T. Takeuchi, J. Am. Chem. Soc. **122**, 5218 (2000)
4. R. Gabai, N. Sallacan, V. Chegel, T. Bourenko, E. Katz, I. Willner, J. Phys. Chem. **105**, 8196 (2001)
5. L. Özcan, Y. Sahin, Sens. Actuators B: Chem. **127**, 362 (2007)
6. J.C.C. Yu, S. Krushkova, E.P.C. Lai, E. Dabek-Zlotorzynska, Anal. Bioanal. Chem **382**(7), 1534 (2005))
7. C. Manitesta, I. Losito, P.G. Zambonin, Anal. Chem. **71**, 1366 (1999)
8. H. Peng, C.D. Liang, A.H. Zhou, Y.Y. Zhang, Q.J. Xie, S.Z. Yao, Anal. Chim. Acta **423**, 221 (2000)
9. H.P. Liao, Z.H. Zhang, H. Li, L.H. Nie, S.Z. Yao, Electrochim. Acta **49**, 4101 (2004)
10. A. Rajasekar, Y.P. Ting, Ind. Eng. Chem. Res. **50**, 2040 (2011)
11. G.L. Wang, J.J. Xu, H.Y. Chen, S.Z. Fu, Biosens. Bioelectron. **25**, 791 (2009)
12. W.W. Tu, Y.T. Dong, J.P. Lei, H.X. Ju, Anal. Chem. **82**, 8711 (2010)
13. N. Haddour, J. Chauvin, C. Gondran, S. Cosnier, J. Am. Chem. Soc. **128**, 9693 (2006)
14. A. Ikeda, M. Nakasu, S. Ogasawara, H. Nakanishi, M. Nakamura, J. Kikuchi, Org. Lett. **11**, 1163 (2009)
15. Z.H. Zhang, Y.J. Yu, P. Wang, ACS Appl. Mater. Interfaces **4**, 990 (2012)
16. D. Tsukamoto, A. Shiro, Y. Shiraishi, Y. Sugano, S. Ichikawa, S. Tanaka, T. Hirai, ACS Catal. **2**, 599 (2012)
17. Y. Tao, C. Wu, D.W. Mazyck, Ind. Eng. Chem. Res. **45**, 5110 (2006)
18. J. Peller, O. Wiest, P.V. Kamat, Environ. Sci. Technol. **37**, 1926 (2003)
19. I. Franch, J. Peral, X. Domenech, J. A. Ayllon, Chem. Commun. 1851 (2005)

20. T.M. Phillips, A.G. Seech, H. Lee, J.T. Trevors, Biodegradation **16**, 363 (2005)
21. T.K. Adhya, S.K. Apte, K. Raghu, N. Sethunathan, N.B. Murthy, Biochem. Biophys. Res. Commun. **221**, 755 (1996)
22. Y. Nagata, Z. Prokop, Y. Sato, P. Jerabek, A. Kumar, Y. Ohtsubo, M. Tsuda, J. Damborsky, Appl. Microbiol. Biotechnol. **71**, 2183 (2005)
23. R. Imai, Y. Nagata, M. Fukuda, M. Takagi, K. Yano, J. Bacteriol. **173**, 6811 (1991)
24. K. Willett, E. Ulrich, R. Hites, Environ. Sci. Technol. **32**, 2197 (1998)
25. T.M. Phillips, A.G. Seech, H. Lee, J.T. Trevors, J. Microbiol. Methods **47**, 181 (2001)
26. Y. Shin, S. Lee, Nano Lett. **8**, 3171 (2008)
27. P. Yang, M. Yang, S. Zou, J. Xie, W. Yang, J. Am. Chem. Soc. **129**, 1541 (2007)
28. D. Chen, Y. Gao, G. Wang, H. Zhang, W. Lu, J. Li, J. Phys. Chem. C **111**, 13163 (2007)
29. P. Gajendran, R. Saraswathi, J. Phys. Chem. C **111**, 11320 (2007)
30. N. Sallacan, M. Zayats, T. Bourenko, A. Kharitonov, I. Willner, Anal. Chem. **74**, 702 (2002)
31. C. Xie, H. Li, S. Li, J. Wu, Z. Zhang, Anal. Chem. **82**, 241 (2010)
32. M. Riskin, R. Tel-Vered, T. Bourenko, E. Granot, I. Willner, J. Am. Chem. Soc. **130**, 9726 (2008)
33. R.N. Liang, D.A. Song, R.M. Zhang, W. Qin, Angewandte Chemie. International Edition **49**, 2556 (2010)
34. E. Brun, G. Marta, R. Puchades, A. Maquieira, J. Agric. Food Chem. **53**, 9352 (2005)
35. C.G. Xie, S. Gao, Q.B. Guo, K. Xu, Microchim. Acta **169**, 145 (2010)
36. D. Du, S. Chen, J. Cai, Y. Tao, H. Tu, A. Zhang, Electrochim. Acta **53**, 6589 (2008)
37. G. Kim, J. Shim, M. Kang, S. Moon, J. Environ. Monit. **10**, 632 (2008)